Spring 5-5-2011

A New Approach for Modeling of a Fluidized Bed by CFD-DEM

Shayan Karimipour
University of Tehran

Navid Mostoufi
University of Tehran, mostoufi@ut.ac.ir

Rahmat Sotudeh-Gharebagh
University of Tehran, sotudeh@ut.ac.ir

H. Chizari
Department of Mechanical Engineering, Universityof Tehran

A NEW APPROACH FOR MODELING OF A FLUIDIZED BED BY CFD-DEM

S. Karimi[1], H. Chizari[2], N. Mostoufi*[1], R. Sotudeh-Gharebagh[1]
[1]Process Design and Simulation Research Center, Department of Chemical Engineering, Universityof Tehran, P.O. Box 11155/4563, Tehran, Iran
[2]Department of Mechanical Engineering, Universityof Tehran, Tehran, Iran
* Corresponding author, Tel.: (+98-21)6696-7797, Fax: (+98-21)6646-1024,
E mail: mostoufi@ut.ac.ir

ABSTRACT
Numerical studies of 3D cylindrical fluidized bed by means of combined computational fluid dynamics (CFD) and discrete element method (DEM) were carried out. For motion of particles, Newton's second law and 3D compressible Navier-Stokes equations in generalized curvilinear coordinates in its conservative form were used. Navier-Stokes equations were solved with high order compact finite difference scheme by fully implicit flux decomposition method. Non-reflecting boundary conditions (NRBC) were used for the outflow boundary. The convergence of this method, especially at high Reynolds number, is significantly better than the SIMPLE method.

INTRODUCTION
Gas-solid fluidized beds have been widely utilized as reactors in the chemical and petrochemical industries. Successful design and operation of fluidized bed reactors requires proper prediction of the performance of reactor. Whereas experiment studies in these systems are quite tedious and expensive, recently modeling of fluidized bed reactors has been extensively used to study these systems. Mathematical models for modeling fluidized bed reactors can be grouped into two main categories: Eulerian-Eulerian (EE) and Lagrangian-Eulerian (LE) .In the EE model, both particles and gas phase are considered as a continuum phase (1, 2, 3 4). Recently, many researchers (5, 6) have adopted the LE model, which is also called discrete element method (DEM), for modeling the phenomena in particle-fluid systems. Using this model, trajectories of individual particles can be traced by solving Newton's second law for each particle while the flow of gas, which is treated as a continuum phase, is described by Navier-Stokes equation.

Finite volume method is usually used to solve the Navier-Stokes equation. The SIMPLE method with staggered grid is suitable for solving Navier-Stokes equation. However, using this method of solution for problems with high Reynolds number is typically unstable. Furthermore, implementing the high order SIMPLE method is so difficult in comparison with finite difference schemes. One of the finite difference methods that can be used for high Reynolds flow is the flux decomposition method. In this method, convective fluxes are decomposed based on eigenvalues which results in a better agreement with the physical properties of the fluid, especially at high Reynolds numbers.

Although the LE approach is more appropriate to study the hydrodynamics of fluidized beds. This model requires large computational resources for large scale systems ($\frac{L}{D} > 4.4Re^{1/6}$ must be chosen to prevent wave reflection). In recent years, non-reflecting boundary conditions (NRBC) were used by some researchers (7, 8) to mitigate wave reflection problems. The concept of NRBC was proposed by Thompson (9) where the idea of specifying the boundary conditions according to the inward and outward propagating waves was introduced. Thompson showing that wave reflections, and therefore, can be used as a fictitious boundary. By using this boundary condition, computational domain and computational time for solving Navier-Stokes equation is decreased. The amount of time saving depends on the gas inlet velocity. As the gas inlet velocity increases the free domain which is required for particles motion increase and therefore the effect of NRBS reduces. But using NRBS almost half the computational time decreases.

In the present work, a CFD-DEM technique was used to investigate the hydrodynamics of a 3D cylindrical fluidized bed. Newton's second law and 3D compressible Navier-Stokes equation in generalized curvilinear coordinates in conservative form was solved for particle and gas phase respectively. In spite of previous studies that usually used SIMPLE method for solving Navier-Stokes equations, these equations were solved with high order compact finite difference scheme by fully implicit flux decomposition method. Using curvilinear coordinates, the physical domain was changed from cylindrical to semi-Cartesian coordinates in computational domain. Furthermore, NRBC was used for outflow boundary to reduce computation time. Hydrodynamics of the bed was investigated and the results were in good agreement with the expected behavior of gas and solids in the fluidized bed.

Governing equations

Equation of motion

In the present work, the flow of sphere particles in a 3D cylindrical fluidized bed was investigated. Newton's second law was applied to each particle. The translational and rotational motion of the particles can be described by following equations (10):

$$m_i = \frac{dV_i}{dt} = f_{f,i} + \sum_{j=1}^{k_i} \left(f_{c,ij} + f_{d,ij}\right) + f_{g,i} \tag{1}$$

$$I_i \frac{d\omega_i}{dt} = \sum_{j=1}^{k_i} T_{i,j} \tag{2}$$

Soft sphere method (11) was used for simulation Inter-particle and particle-wall contact forces.

For the gas phase, three-dimensional compressible Navier-Stokes equations in generalized curvilinear coordinates (ξ, η, ζ)were written in conservative form:

$$\frac{\partial \varepsilon Q}{\partial t} + \frac{\partial (E - E_v)}{\partial \xi} + \frac{\partial (F - F_v)}{\partial \eta} + \frac{\partial (G - G_v)}{\partial \zeta} = P \tag{3}$$

$$Q=\frac{1}{J}\begin{pmatrix}\rho\\ \rho u\\ \rho v\\ \rho w\\ E_t\end{pmatrix}\quad E=\frac{1}{J}\begin{pmatrix}\rho U\varepsilon\\ \rho U u\varepsilon+P\xi_x\\ \rho U v\varepsilon+P\xi_y\\ \rho U w\varepsilon+P\xi_z\\ U(E_t+P)\varepsilon+U_P P(1-\varepsilon)\end{pmatrix}\quad F=\frac{1}{J}\begin{pmatrix}\rho V\varepsilon\\ \rho V u\varepsilon+P\eta_x\\ \rho V v\varepsilon+P\eta_y\\ \rho V w\varepsilon+P\eta_z\\ V(E_t+P)\varepsilon+V_P P(1-\varepsilon)\end{pmatrix}$$

$$G=\frac{1}{J}\begin{pmatrix}\rho W\varepsilon\\ \rho W u\varepsilon+P\zeta_x\\ \rho W v\varepsilon+P\zeta_y\\ \rho W w\varepsilon+P\zeta_z\\ W(E_t+P)\varepsilon+W_P P(1-\varepsilon)\end{pmatrix}\quad E_v=\frac{1}{J}\begin{pmatrix}0\\ \varepsilon(\tau_{xx}\xi_x+\tau_{xy}\xi_y+\tau_{xz}\xi_z)\\ \varepsilon(\tau_{yx}\xi_x+\tau_{yy}\xi_y+\tau_{yz}\xi_z)\\ \varepsilon(\tau_{zx}\xi_x+\tau_{zy}\xi_y+\tau_{zz}\xi_z)\\ Q_x\xi_x+Q_y\xi_y+Q_z\xi_z\end{pmatrix}$$

$$F_v=\frac{1}{J}\begin{pmatrix}0\\ \varepsilon(\tau_{xx}\eta_x+\tau_{xy}\eta_y+\tau_{xz}\eta_z)\\ \varepsilon(\tau_{yx}\eta_x+\tau_{yy}\eta_y+\tau_{yz}\eta_z)\\ \varepsilon(\tau_{zx}\eta_x+\tau_{zy}\eta_y+\tau_{zz}\eta_z)\\ Q_x\eta_x+Q_y\eta_y+Q_z\eta_z\end{pmatrix}\quad G_v=\frac{1}{J}\begin{pmatrix}0\\ \varepsilon(\tau_{xx}\zeta_x+\tau_{xy}\zeta_y+\tau_{xz}\zeta_z)\\ \varepsilon(\tau_{yx}\zeta_x+\tau_{yy}\zeta_y+\tau_{yz}\zeta_z)\\ \varepsilon(\tau_{zx}\zeta_x+\tau_{zy}\zeta_y+\tau_{zz}\zeta_z)\\ Q_x\zeta_x+Q_y\zeta_y+Q_z\zeta_z\end{pmatrix} \tag{4}$$

$$P=\frac{1}{J}\begin{pmatrix}0\\ S_1F_\xi\\ S_1F_\eta\\ S_1F_\zeta\\ S_2(F_\xi U_P+F_\eta V_P+F_\zeta W_P)+S_2Q_P\end{pmatrix},\quad S_1=\frac{L_\infty}{\rho_\infty U_\infty^2},\quad S_2=\frac{L_\infty}{\rho_\infty U_\infty^3},$$

The contra-variant velocity components U, V, and W are defined as:

$$U=u\xi_x+v\xi_y+w\xi_z,\quad V=u\eta_x+v\eta_y+w\eta_z,\quad W=u\zeta_x+v\zeta_y+w\zeta_z, \tag{5}$$

Other equations used in Navier-Stokes equations are introduced as follow:

$$\begin{cases}Q_x=-q_x+\varepsilon(u\tau_{xx}+v\tau_{xy}+w\tau_{xz})\\ Q_y=-q_y+\varepsilon(u\tau_{yx}+v\tau_{yy}+w\tau_{yz})\\ Q_z=-q_z+\varepsilon(u\tau_{zx}+v\tau_{zy}+w\tau_{zz})\end{cases} \tag{6}$$

$$Q_P=\frac{1}{V_{cell}}\sum h(4\pi r_P^2)(T_P-\tilde{T}),\quad \tilde{T}=T\times T_\infty,\quad h=\frac{Nu\times\tilde{k}}{2r_P},\quad \tilde{k}=k\times k_\infty, \tag{7}$$

$$F_\xi=\frac{F_x\xi_x+F_y\xi_y+F_z\xi_z}{\sqrt{\xi_x^2+\xi_y^2+\xi_z^2}},\quad F_\eta=\frac{F_x\eta_x+F_y\eta_y+F_z\eta_z}{\sqrt{\eta_x^2+\eta_y^2+\eta_z^2}}\quad F_\zeta=\frac{F_x\zeta_x+F_y\zeta_y+F_z\zeta_z}{\sqrt{\zeta_x^2+\zeta_y^2+\zeta_z^2}} \tag{8}$$

$$\tau_{ij}=\frac{\mu}{Re}\left\{\left(\frac{\partial u_i}{\partial x_j}+\frac{\partial u_j}{\partial x_i}\right)-\frac{2}{3}\delta_{ij}\frac{\partial u_k}{\partial x_k}\right\},\quad q_i=-\frac{k_{eff}}{ReM_r^2Pr(\gamma-1)}\frac{\partial T}{\partial x_i} \tag{9}$$

$$k_{eff}=\frac{\tilde{k}\varepsilon+\tilde{k}_P(1-\varepsilon)}{k_\infty} \tag{10}$$

For solving Navier-Stokes equations with flux decomposition method, first the Jacobean matrices must be evaluated:

$$A_{ij}=\frac{\partial E_i}{\partial Q_j},\quad B_{ij}=\frac{\partial F_i}{\partial Q_j},\quad C_{ij}=\frac{\partial G_i}{\partial Q_j} \tag{11}$$

By considering$Q^{n+1} = Q^p + \delta Q^p$ Navier-Stokes equations are changed to:

$$\varepsilon^{n+1}\left(\frac{\partial Q}{\partial t}\right)^{n+1} + Q^{n+1}\left(\frac{\partial \varepsilon}{\partial t}\right)^{n+1} + \frac{\partial A}{\partial \xi}\delta Q^p + \frac{\partial B}{\partial \eta}\delta Q^p + \frac{\partial C}{\partial \zeta}\delta Q^p = P^n + \left(\frac{\partial E_v}{\partial \xi} + \frac{\partial F_v}{\partial \eta} + \frac{\partial G_v}{\partial \zeta}\right)^n - \left(\frac{\partial E}{\partial \xi} + \frac{\partial F}{\partial \eta} + \frac{\partial G}{\partial \zeta}\right)^n \quad (12)$$

The Jacobean matrices are decomposed using eigenvalues (λ):

$$A = A^+ + A^- \quad A^{\pm} = \frac{1}{2}(A \pm \lambda I) \quad (13)$$

$$\frac{\partial A^+}{\partial \xi} = A^+_{i,j,k} - A^+_{i-1,j,k}, \quad \frac{\partial A^-}{\partial \xi} = A^-_{i+1,j,k} - A^-_{i,j,k} \quad (14)$$

Finally, flow field obtain by solving following equation:

$$\left\{I + \frac{2\Delta t}{6\varepsilon^{n+1} - 4\varepsilon^n + \varepsilon^{n-1}}\left(\frac{\partial A}{\partial \xi} + \frac{\partial B}{\partial \eta} + \frac{\partial C}{\partial \zeta}\right)\right\}\delta Q^p = R_{imp}$$

$$R_{imp} = -\frac{\varepsilon^{n+1}(3Q^p - 4Q^n + Q^{n-1}) + Q^p(3\varepsilon^{n+1} - 4\varepsilon^n + \varepsilon^{n-1})}{6\varepsilon^{n+1} - 4\varepsilon^n + \varepsilon^{n-1}} - \frac{2\Delta t}{6\varepsilon^{n+1} - 4\varepsilon^n + \varepsilon^{n-1}}\left\{\frac{\partial (E - E_v)}{\partial \xi} + \frac{\partial (F - F_v)}{\partial \eta} + \frac{\partial (G - G_v)}{\partial \zeta}\right\} + \frac{2\Delta t}{6\varepsilon^{n+1} - 4\varepsilon^n + \varepsilon^{n-1}}P \quad (15)$$

NON-REFLECTING BOUNDARY CONDITIONS

If Q is the conservative variable,q is the primitive variable and M is the conversion matrix as below:

$$M = \frac{\partial Q}{\partial q} = \begin{pmatrix} 1 & 0 & 0 & 0 & 0 \\ u & \rho & 0 & 0 & 0 \\ v & 0 & \rho & 0 & 0 \\ w & 0 & 0 & \rho & 0 \\ \frac{1}{2}(u^2 + v^2 + w^2) & \rho u & \rho v & \rho w & \frac{1}{\gamma - 1} \end{pmatrix}, \quad q = \begin{pmatrix} \rho \\ u \\ v \\ w \\ P \end{pmatrix} \quad (16)$$

NRBC in the ξ-direction in conservative form can be written as

$$\frac{\partial Q}{\partial t} + D_i + M\bar{\bar{b}}\frac{\partial q}{\partial \eta} + M\bar{\bar{c}}\frac{\partial q}{\partial \zeta} = JR_v \quad (17)$$

where

$$\bar{\bar{b}} = \begin{pmatrix} V & \rho\eta_x & \rho\eta_y & \rho\eta_z & 0 \\ 0 & V & 0 & 0 & \frac{\eta_x}{\rho} \\ 0 & 0 & V & 0 & \frac{\eta_y}{\rho} \\ 0 & 0 & 0 & V & \frac{\eta_z}{\rho} \\ 0 & \gamma P\eta_x & \gamma P\eta_y & \gamma P\eta_z & V \end{pmatrix}, \quad \bar{\bar{c}} = \begin{pmatrix} W & \rho\zeta_x & \rho\zeta_y & \rho\zeta_z & 0 \\ 0 & W & 0 & 0 & \frac{\zeta_x}{\rho} \\ 0 & 0 & W & 0 & \frac{\zeta_y}{\rho} \\ 0 & 0 & 0 & W & \frac{\zeta_z}{\rho} \\ 0 & \gamma P\zeta_x & \gamma P\zeta_y & \gamma P\zeta_z & W \end{pmatrix} \quad (18)$$

$$D = Md = \begin{pmatrix} D_1 \\ D_2 \\ D_3 \\ D_4 \\ D_5 \end{pmatrix} = \begin{pmatrix} d_1 \\ ud_1 + \rho d_2 \\ vd_1 + \rho d_3 \\ wd_1 + \rho d_4 \\ \frac{1}{2}(u^2 + v^2 + w^2)d_1 + \rho u d_2 + \rho v d_3 + \rho w d_4 + \frac{d_5}{\gamma - 1} \end{pmatrix} \tag{19}$$

$$d = PL = \begin{pmatrix} d_1 \\ d_2 \\ d_3 \\ d_4 \\ d_5 \end{pmatrix} = \begin{pmatrix} \tilde{\xi}_x L_1 + \tilde{\xi}_y L_2 + \tilde{\xi}_z L_3 + \frac{\rho}{\sqrt{2}c}(L_4 + L_5) \\ -\tilde{\xi}_z L_2 + \tilde{\xi}_y L_3 + \frac{\tilde{\xi}_x}{\sqrt{2}}(L_4 - L_5) \\ \tilde{\xi}_z L_1 - \tilde{\xi}_x L_3 + \frac{\tilde{\xi}_y}{\sqrt{2}}(L_4 - L_5) \\ -\tilde{\xi}_y L_1 + \tilde{\xi}_x L_2 + \frac{\tilde{\xi}_z}{\sqrt{2}}(L_4 - L_5) \\ \frac{\rho c}{\sqrt{2}}(L_4 + L_5) \end{pmatrix} \tag{20}$$

$$L = \begin{pmatrix} L_1 \\ L_2 \\ L_3 \\ L_4 \\ L_5 \end{pmatrix} = \begin{pmatrix} U\left(\tilde{\xi}_x \frac{\partial \rho}{\partial \xi} + \tilde{\xi}_z \frac{\partial v}{\partial \xi} - \tilde{\xi}_y \frac{\partial w}{\partial \xi} - \frac{\tilde{\xi}_x}{c^2}\frac{\partial P}{\partial \xi}\right) \\ U\left(\tilde{\xi}_y \frac{\partial \rho}{\partial \xi} - \tilde{\xi}_z \frac{\partial u}{\partial \xi} + \tilde{\xi}_x \frac{\partial w}{\partial \xi} - \frac{\tilde{\xi}_y}{c^2}\frac{\partial P}{\partial \xi}\right) \\ U\left(\tilde{\xi}_z \frac{\partial \rho}{\partial \xi} + \tilde{\xi}_y \frac{\partial u}{\partial \xi} - \tilde{\xi}_x \frac{\partial v}{\partial \xi} - \frac{\tilde{\xi}_z}{c^2}\frac{\partial P}{\partial \xi}\right) \\ (U + C)\left(\frac{\tilde{\xi}_x}{\sqrt{2}}\frac{\partial u}{\partial \xi} + \frac{\tilde{\xi}_y}{\sqrt{2}}\frac{\partial v}{\partial \xi} + \frac{\tilde{\xi}_z}{\sqrt{2}}\frac{\partial w}{\partial \xi} + \frac{1}{\sqrt{2}\rho c}\frac{\partial P}{\partial \xi}\right) \\ (U - C)\left(-\frac{\tilde{\xi}_x}{\sqrt{2}}\frac{\partial u}{\partial \xi} - \frac{\tilde{\xi}_y}{\sqrt{2}}\frac{\partial v}{\partial \xi} - \frac{\tilde{\xi}_z}{\sqrt{2}}\frac{\partial w}{\partial \xi} + \frac{1}{\sqrt{2}\rho c}\frac{\partial P}{\partial \xi}\right) \end{pmatrix} \tag{21}$$

RESULTS AND DISCUSSION

In this numerical study, a cylindrical fluidized bed with 7.5 cm diameter and 50 cm height, filled with 10000 particles was considered. The diameter and density of particles were 2 mm and 1100 kg/m^3, respectively. A jet of gas was introduced into the bed via a central hole with jet velocity of 8 m/s ($u \sim 5u_{mf}$).

Fig. 1 shows snapshots of particles positions in the bed. As can be seen in this figure, particles that are at the center of the bed accelerate very fast and move vertically in the bed. The initial acceleration of the particles is so high that they travel almost 50 cm in the bed. This high acceleration is due to the high vertical drag force exerted on particles due to high gas velocity in the central area of the bed. However, particles in the annulus of this area do not move very noticeably in the vertical direction. This is mainly due to the low gas velocity in this region. The gas velocity in this region is low for two reasons. First, the gas is not introduced into the bed from near the walls. Second, wall effects induce a velocity boundary layer in which the gas velocity is low near the wall.

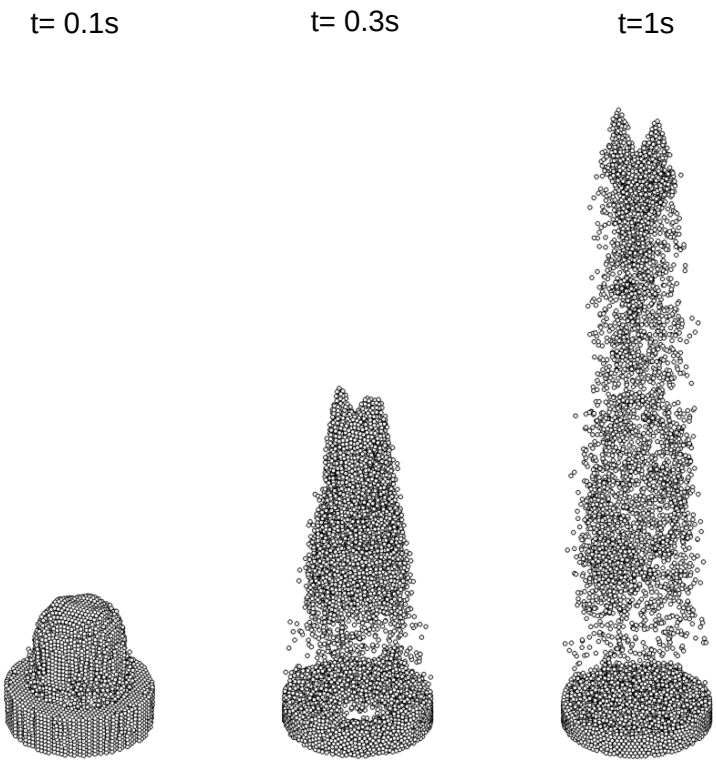

Fig.1. Snapshot of particle motion

Over time by particles movement from distributor, the void fraction in that region increase and the gas velocity decrees. Void fraction increasing in distributor center is more than the distributor corner. So reduction in the gas velocity in the distributor center holes is more than distributor corners. The gas velocity affects particles motion that caused to occurring two peaks in particles motion. If the simulation has been permitted to continue for a longer time, the transient state of the bed would have been vanished and a better solid flow pattern would have been obtained. Since the time required for the calculation is very high (around 1 month), this results has not been obtained yet.

Fig. 2 shows velocity vector and density contour of the gas in the bed. The bed is divided into four sections that are perpendicular to each other to able to show the behavior of the flow field in 3D cylindrical bed. However, this figure shows only two sections of the bed.

For low Mach number flows, changes in density are low, but as it can be seen in these figures, with upcoming the particles the density of fluid before them increases. Moreover, the velocity vectors in center of the cylinder are high. This flow pattern is in accordance with a gas flow pattern in a cylinder with boundary layer. According to the continuity relation, while the gas velocity increases, the density of gas decreases. This result shows that the presented model and the implemented method can predict compressibility behavior of the gas very well.

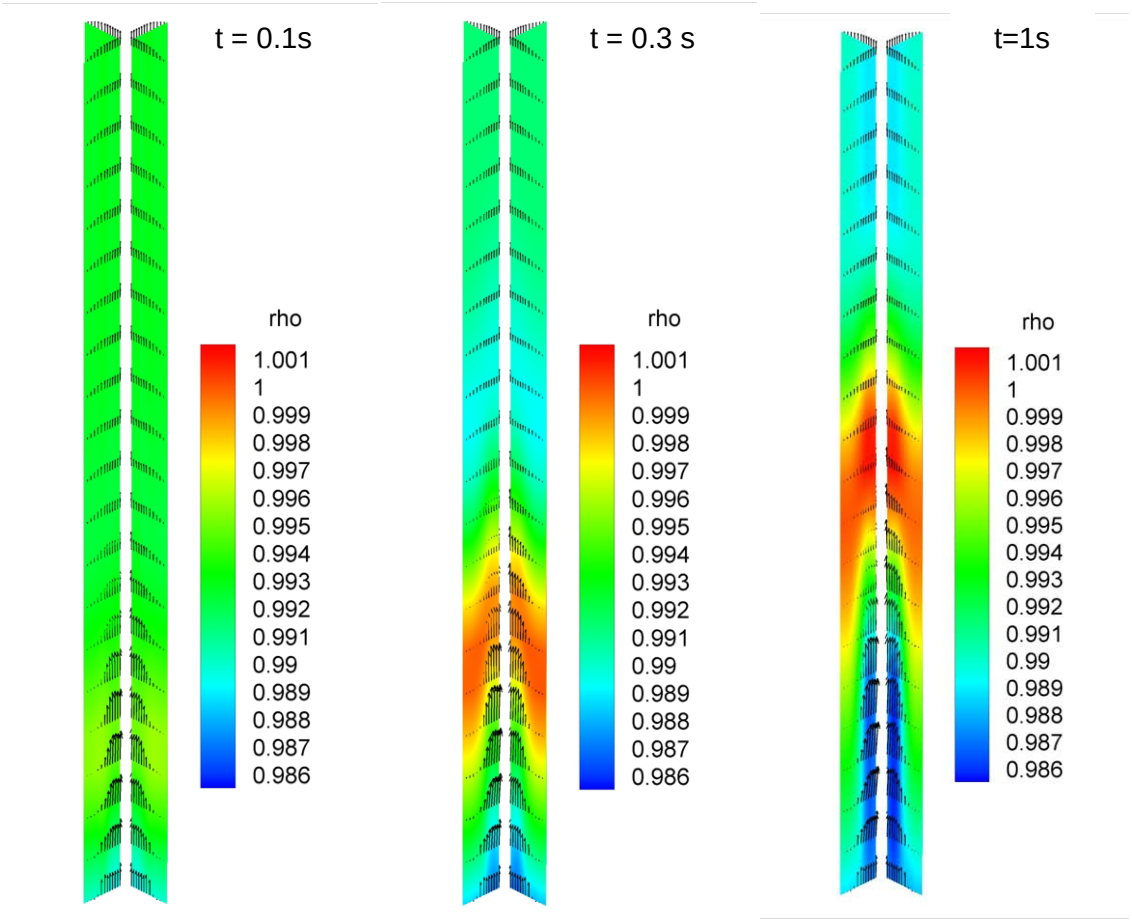

Fig.2.velocity vectors and density contour of gas

CONCLUSIONS

A combination of CFD and DEM was used to study the behavior of the high velocity fluidized bed reactor. The conservative form of Navier-Stocks equations in curvilinear coordinate was derived and used to obtain flow field of the gas in the bed. As described before, flux decomposition method is more compatible with high Reynolds numbers and high order solving methods than SIMPLE method; therefore in this work flux decomposition method was used for modeling high Reynolds fluidized bed. It must be emphasized that solving high order Navier-Stokes equations caused to seeing the physical behavior of the bed much better.

NOTATION

d	amount of wave for each primitive Navier-Stokes equation
D	amount of wave for each conservative Navier-Stokes equations
E	inviscid flux vector (ξ direction)
E_v	viscous flux vector (ξ direction)
f_c	contact force, N
f_d	Damping force, N
f_f	particle-fluid interaction force, N
f_g	acceleration force, N
F	inviscid flux vector (η direction)

F_v viscous flux vector (η direction)
G inviscid flux vector (ζ direction)
G_v viscous flux vector (ζ direction)
I moment of inertia, kg m^2
J Jacobian of the coordinate transformation,
L amount of each characteristic wave
M conversion matrix
q vector of primitive variables
Q vector of conservative variables
U contra-variant velocity(x direction), m s^{-1}
V contra-variant velocity(y direction) , m s^{-1}
W contra-variant velocity(z direction) , m s^{-1}

REFERENCES

1. D. Gidaspow, Y. C. Seo, B. Ettehadieh, Hydrodynamics of fluidization: Experimental and theoretical bubble sizes in a two-dimensional bed with a jet, *Chemical Engineering Communication*, 22,253-272, 1983.
2. J. A. M. Kuipers, K. J. vanDuin, F. P. H. van Beckum, W. P. M. van Swaaij, Computer simulation of the hydrodynamics of a two-dimensional gas-fluidized bed, *Computer and Chemical Engineering*, 17(8), 839-858,1993.
3. C. Guenther and M. Syamlal, The effect of numerical diffusion on simulation of isolated bubbles in a gas-solid fluidized bed, *Powder Technology*,116, 142-154, 2001.
4. F. Gevrin, O. Masbernat, O. Simonin, Granular pressure and particle velocity fluctuations prediction in liquid fluidized bed*, Chemical Engineering Science,* 63, 2450-2464, 2008.
5. H. P. Zhu, Z.Y. Zhou, R. Y. Yang, A. B. Yu, Discrete particle simulation of particulate systems: a review of major application and findings, *Chemical Engineering Science,* 63(23), 5728-5770, 2008.
6. M. Ye, M. A. van der Hoef, J. A. M. Kuipers, A numerical study of fluidization behavior of Geldart A particles using a discrete particle model, *Powder Technology,* 139, 129, 2003.
7. L. H. Jiang, Shan, C. Liu, M. Visbal, Non-Reflecting Boundary Conditions For DNS in Curvilinear Coordinates, International Conference, Rutgers, New Jersey, June 7-9.1999.
8. T. J. Poinsot, and S. K. Lele, Boundary Conditions for Direct Simulations of Compressible Viscous Floes, *Journal of Computational Physics*, 101, 104-129, 1992.
9. K. W. Thompson, Time-Dependent Boundary Conditions for Hyperbolic Systems II, *Journal of Computational Physics*, 89, 439-461, 1990.
10. B.H. Xu and A. B. Yu, Numerical simulation of the gas-solid flow in a fluidized bed by combining discrete particle method with computational fluid dynamics, *Chemical Engineering Science*, 52 (16), 2785-2809,1997.
11. P. A. Cundall and O. D. L. Strack, A discrete numerical model for granular assemblies, *Geotechnique,* 29, 47-65, 1979.